

Towards a model for aerosol removal by rain scavenging: The role of physical-chemical characteristics of raindrops

Fernanda Oduber^a, Ana Isabel Calvo^{a,*}, Carlos Blanco-Alegre^a, Amaya Castro^a, Celia Alves^b, Mario Cerqueira^b, Franco Lucarelli^c, Silvia Nava^c, Giulia Calzolari^c, Javier Martin-Villacorta^a, Valdemar Esteves^d, Roberto Fraile^a

^a Department of Physics, IMARENAB, University of León, León, Spain

^b Department of Environment and Marine Studies, CESAM, University of Aveiro, Aveiro, Portugal

^c Department of Physics and Astronomy, University of Florence and INFN-Florence, Florence, Italy

^d Department of Chemistry, CESAM, University of Aveiro, Aveiro, Portugal

ARTICLE INFO

Article history:

Received 15 July 2020

Received in revised form 14 November 2020

Accepted 16 December 2020

Available online xxx

Keywords

Aerosol

Disdrometer

Linear model

Removal coefficients

Precipitation

ABSTRACT

A one-year study was carried out in León, Spain, in order to characterize physically and chemically the precipitation. With the aim of studying the scavenging process of atmospheric pollutants, scavenging ratio and removal coefficients were calculated through physical parameters of raindrops (obtained by disdrometer data) and through chemical properties of aerosols. Finally, linear models for the prediction of the chemical composition of rainwater and the efficiency of the removal effect were established. In general, the rainwater was dominated by $\text{NH}_4^+ > \text{SO}_4^{2-} > \text{NO}_3^-$ in all seasons. Higher ion concentrations and conductivity, and lowest pH were observed in summer, due to the low volume of rain. In winter, the high values of Na^+ and Cl^- in the rainwater show the contribution from marine sources, while in summer the high concentrations of Ca^{2+} , Mg^{2+} , SO_4^{2-} , NH_4^+ and NO_3^- reflected the contribution from both crustal and anthropogenic sources. The linear models show that the amount of dissolved organic carbon and of the water-soluble ions on rain samples, Ca^{2+} , SO_4^{2-} , NO_3^- , increases with the volume swept by the falling drops. Insoluble carbon fraction has a negative dependence with the volume swept and positive with the diameter of the raindrop. Removal coefficients are affected by the concentration in the air of each species before precipitation, the duration of the event and the time elapsed between two precipitation events.

© 2020

1. Introduction

Over years, several authors have highlighted the negative impact of air pollutants on human health and the environment (Bernstein et al., 2004; Kampa and Castanas, 2008; Ren-Jian et al., 2012), especially in megacities (Lelieveld et al., 2015; Mage et al., 1996; Naddafi et al., 2012). Atmospheric wet deposition plays a crucial role in mitigating these negative effects, as it acts directly on the removal and transport of different pollutants and soluble gases from the atmosphere to the earth's surface (Keresztesi et al., 2017; Seinfeld and Pandis, 2016), through two main processes: in-cloud and below-cloud scavenging. Below-cloud scavenging depends on the characteristics of rainfall (raindrop size distribution and rainfall rate) and on the local/regional concentration of the particles and gases in the atmosphere and in-cloud processes involve both, the condensation of water vapor onto

aerosols and the incorporation of gases by reactions in the aqueous phase (Celle-Jeanton et al., 2009; Xu et al., 2017).

The study of the chemical properties of rainwater, and of the concentration and composition of the aerosol, provides useful information on the emissions of pollutants, since it helps to identify the possible sources that contribute to rainwater chemistry, local and regional dispersion of pollutants and their impact on the ecosystem (Martins et al., 2019; Sanets and Chuduk, 2005; Zhang et al., 2007). The composition of rainwater depends on several factors, such as the local and long-range emissions sources, geography and meteorological conditions (Alastuey et al., 1999; Calvo et al., 2012; Jain et al., 2019; Knote et al., 2015; Mori et al., 2014).

The scavenging process of different species is affected by the intensity and volume of precipitation (Calvo et al., 2012; Custódio et al., 2014; Luan et al., 2019; Pan and Wang, 2015; Uchiyama et al., 2017). However, there are many other parameters involved in this process, such as concentration, size distribution and composition of atmospheric aerosol and raindrop size distribution (Blanco-Alegre et al., 2019, 2018; Fredericks and Saylor, 2019; Zikova and Zdimal, 2016). In recent years, several authors have proposed different

* Corresponding author.

E-mail address: aicalg@unileon.es (A.I. Calvo)

models to explain the removal process of aerosols by rain. For example, Olszowski and Ziemcik (2018) presented a linear model for the reduction of PM_{10} mass concentrations, which includes the type of precipitation and the water vapor content in air. Moreover, Roy et al. (2019), proposed a linear model to predict the aerosol scavenging, based on the influence of rain rate and duration. In previous studies, carried out in León, Spain, the influence of the physical characteristics of precipitation on the total concentration of particles (Castro et al., 2010) and on the removal of black carbon (Blanco-Alegre et al., 2019), have already been reported. However, studies integrating the chemical properties of aerosol and precipitation and the physical properties of precipitation are scarce, underestimating the potential synergies between them. Studies involving the physical-chemical parameters of precipitation can provide valuable information to deepen the understanding of the process of aerosol removal by rainfall.

The hypothesis that supports our study is that the scavenging of aerosols is a function of the chemical properties of the aerosol and the physical characteristics of rain. In order to verify such hypothesis, a one-year sampling campaign of aerosols and precipitation was carried out in León (NW Spain), with the aim of: (i) studying the chemical and physical characteristics of precipitation and identifying the main weather types associated with them; (ii) studying the influence of the aerosol chemical composition and the physical characteristics of precipitation on the removal processes, through the scavenging ratio and removal coefficients; and (iii) establishing several linear models to explain the removal process of the different chemical species in the air, from the physical properties of rainwater and aerosol chemical composition.

2. Experimental

2.1. Sampling site

The sampling campaign was carried out in León city, located in the NW of the Iberian Peninsula ($42^{\circ} 36' N$, $05^{\circ} 35' W$ and 838 m above sea level) (Fig. 1). León is mainly a residential city, with a population of 125,317 inhabitants (2017 report of the National Institute for Statistics www.ine.es) and characterized by the absence of large air-emitting industries and by a high contribution of air emissions from traffic and small-scale heating devices, especially during the cold months (Oduber et al., 2018). The climate is continental type with Mediterranean influences. The winters are long and cold with daily mean temperatures

of $5^{\circ}C$, and summers are warm with mean temperatures of $20^{\circ}C$. On average, there are 2624 sun hours, 78 rain days and 16 storm days per year, with frequent frosts in winter (74 frost days per year, on average), and a mean of 16 snow days. Summer droughts are very common, with sporadic storm events, often with hail (Fernández-Raga et al., 2017). According to the Spanish National Agency for Meteorology (AEMET in its Spanish acronym), the average seasonal rainfall in León ranges from 27 mm (summer) to 62 mm (autumn), with 58 mm in winter and 44 mm in spring.

2.2. Material and methods

2.2.1. PM_{10} and rainwater sampling

The sampling was carried out on the terrace of the Faculty of Veterinary Sciences of the University of León, located in a suburban area in the NE of the urban center. The campaign ran between 09 March 2016 and 14 March 2017. In order to analyze the evolution of the data along the year, seasons have been defined as follows: i) winter: from 21 December to 20 March; ii) spring: from 21 March to 20 June; iii) summer: from 21 June to 20 September; and iv) autumn: from 21 September to 20 December.

Weather information (temperature, wind and relative humidity) was obtained from a weather station installed in the sampling point. The origin of air masses during the study period was estimated by the HYSPLIT model (Draxler and Rolph, 2012; Rolph et al., 2017; Stein et al., 2015) through the determination of 3-day back trajectories (at 500, 1500 and 3000 m).

During the sampling period, a total of 74 rainwater samples and a total of 739 PM_{10} samples (369 quartz filters and 370 teflon filters) were collected. The filters and rainwater samples were collected every 24 h, starting at 1200 UTC every day.

The sampling of PM_{10} was carried out using a low volume sampler (TECORA, ECHOPM) equipped with 47 mm diameter teflon filters and using a high volume sampler (CAV-Mb) equipped with 150 mm diameter quartz filters. PM_{10} mass was determined by gravimetry, using an electronic semi-microbalance (Mettler Toledo, XPE105DR).

Rainwater samples were collected in glass bottles using a wet-only precipitation sampler (Eigenbrodt UNS 130/E). Conductivity and pH of precipitation samples were determined immediately after collection. Then, the water samples were filtered through a 15 mm diameter quartz filters in order to separate the insoluble and soluble fractions.

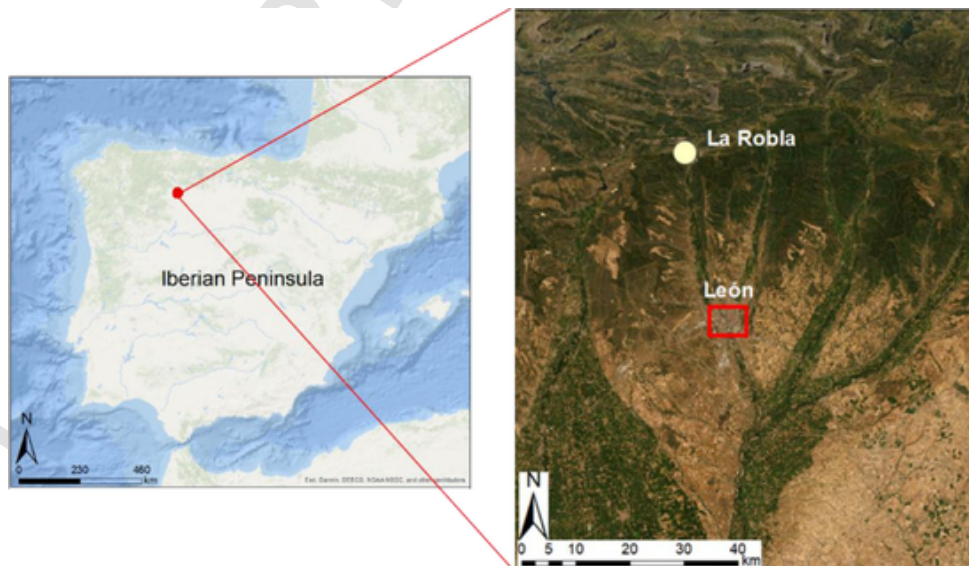


Fig. 1. Location of León and La Robla in the Iberian Peninsula. The green area shows vegetation zones.

2.2.2. PM_{10} and rainwater analysis

The thermo-optical technique was used for the determination of organic and elemental carbon (OC and EC) of quartz filters of PM_{10} , and for the determination of water insoluble organic and elemental carbon (WIOC and WIEC) of the insoluble rainwater fraction, following the methodology described by Custódio et al. (2014) and Pio et al. (2011).

Teflon filters were used for the analysis of water-soluble inorganic ions by ionic chromatography, and for the determination of major trace elements, using PIXE technique (Particle-Induced X-ray Emission) (Lucarelli et al., 2015), following the methodology described by Oduber et al. (2019a).

The soluble fractions of rainwater samples were separated into two fractions; one of them was used for the determination of dissolved organic carbon (DOC) content. This analysis was carried out by combustion and infrared detection in a Total Organic Carbon Analyzer Shimadzu (TOC-VCPH). The other fraction was filtered through a 13 mm polyvinyl difluoride (PVDF) syringe filter with 0.2 μm pore size (WhatmanTM) and used for the determination of the water-soluble inorganic ions by ionic chromatography. The chromatographic analysis was performed on a Thermo Scientific DionexTM ICS-5000 equipment provided with an IonPac[®] CS16 column (4 × 250 mm) and an IonPac[®] AS11 column (4 × 250 mm) for the analysis of cations (Li^+ , Na^+ , K^+ , Ca^{2+} , Mg^{2+} , NH_4^+) and anions (F^- , Cl^- , SO_4^{2-} , NO_3^- , NO_2^-), respectively.

2.2.3. Disdrometer

The raindrop size spectrum was obtained with a laser disdrometer (Laser Precipitation Monitor, LPM) of *Thies Clima*, which registered drops between 0.125 and 8 mm in 22 drop size ranges, on a 1-minute basis (Fernández-Raga et al., 2009). The LPM was operational throughout the entire campaign; thus, when a precipitation event occurred, the raindrop characteristics were recorded during the entire event. The LPM was placed 3 m far from the rain collector and close to the aerosol samplers (all of them on the same terrace of the Faculty of Veterinary Sciences of the University of León). As a consequence, the characteristics of rainwater are supposed to be similar at all installed sampling equipment. From the data provided by the LPM, the following rainfall variables were obtained: precipitation intensity, accumulated precipitation, number of drops, volume swept by falling drops, mean and standard deviation of raindrop sizes.

2.2.4. Circulation weather types

In order to study the relationship between the precipitation and the weather type, a Circulation Weather Types (CWTs) classification, based on Lamb (1972), was carried out. Four indices associated with the direction and vorticity of geostrophic flow (southerly flow SF, westerly flow WF, southerly shear vorticity ZS and westerly shear vorticity ZW)

have been calculated from the surface pressure in 16 grid points distributed over the Iberian Peninsula (Trigo and DaCamara, 2000; Fernández-Raga et al., 2017). They have been used to establish each of the 26 different CWTs (Table 1).

2.2.5. Statistical analysis

The statistical treatment has been carried out using SPSS software (IBM Statistics Software V. 24). The Kruskal-Wallis non-parametric test (Kruskal and Wallis, 1952) followed by Dunn test (Dunn, 1964), were applied to the data in order to identify statistically significant differences. The correlations were calculated using the nonparametric Pearson's rank correlation method. The principal component analysis (PCA) was performed, applying a matrix of Varimax rotated components to the studied species, in order to determinate a common origin (Hastie et al., 2009). The application of an automatic linear modeling (IBM SPSS Statistics 24) by step-wise, with an entry probability of 0.05 was also used.

2.2.6. Volume-weighted mean precipitation concentrations

Volume-weighted mean concentrations (VWM, in $\mu\text{eq L}^{-1}$) of ionic species in rainwater have been calculated using Eq. (1):

$$VWM = \left(\sum_{i=1}^N C_i P_i \right) / \sum_{i=1}^N P_i \quad (1)$$

where C_i is the concentration of each species in $\mu\text{eq L}^{-1}$, P_i the precipitation amount for each precipitation event, and N the total number of precipitation events in each study period.

2.2.7. Neutralization factors and enrichment factors

Neutralization factors (NF , dimensionless) have been calculated following Eq. (2) (Kulshrestha et al., 1995):

$$NF_x = C_x / \left[C_{\text{SO}_4^{2-}} + C_{\text{NO}_3^-} \right] \quad (2)$$

where C_x is the concentration of the species of interest and $C_{\text{SO}_4^{2-}}$ and $C_{\text{NO}_3^-}$ are the concentrations of sulfate and nitrate in rainwater, respectively. All ion concentrations are expressed in $\mu\text{eq L}^{-1}$.

The enrichment factors (EF , dimensionless) were calculated for both the seawater and crustal material, according to Eq. (3) (Kulshrestha et al., 1996; Zhang et al., 2007):

$$EF = \frac{(C_x/C_r)_{\text{sample}}}{(C_x/C_r)_{\text{crustal/seawater}}} \quad (3)$$

where $(C_x/C_r)_{\text{sample}}$ is the ratio between the concentration of an element x and that of a reference element (r) in the sample. $(C_x/C_r)_{\text{crustal/seawater}}$ is the ratio between the same elements but consid-

Table 1
Original weather types CWTs, with 2 pure types controlled by geostrophic vorticity (A and C), 8 directional types and 16 hybrid types.

Lamb's weather types							
Pure	Directional types		Cyclonic hybrid		Anticyclonic hybrid		
C	Cyclonic	NE	Northeasterly	CNE	Cyclonic northeasterly	ANE	Anticyclonic northeasterly
A	Anticyclonic	E	Easterly	CE	Cyclonic easterly	AE	Anticyclonic easterly
		SE	Southeasterly	CSE	Cyclonic southeasterly	ASE	Anticyclonic southeasterly
		S	Southerly	CS	Cyclonic southerly	AS	Anticyclonic southerly
		SW	Southwesterly	CSW	Cyclonic southwesterly	ASW	Anticyclonic southwesterly
		W	Westerly	CW	Cyclonic westerly	AW	Anticyclonic westerly
		NW	Northwesterly	CNW	Cyclonic northwesterly	ANW	Anticyclonic northwesterly
		N	Northerly	CN	Cyclonic northerly	AN	Anticyclonic northerly

ering the concentrations in the seawater or crustal material (Keene et al., 1986; Zhang et al., 2007).

In order to determine the best seawater tracer, the Mg^{2+}/Na^+ ratio was evaluated. A ratio higher than 0.227 indicates a crustal Mg^{2+} influence and a lower ratio suggests a crustal Na^+ origin (Jordan et al., 2003). In this study, the mean Mg^{2+}/Na^+ ratio was 0.713 and, according to this result, sodium was used as seawater reference element. Following Zhang et al. (2007), calcium was used as crustal reference, since it is a typical lithophylic element representative of the soil composition.

Besides, the source contribution of seawater and crustal was obtained as follows (Zhang et al., 2007):

$$\text{Seawater fraction \%} = 100(C_x/C_{Na^+})_{\text{seawater}} / (C_x/C_{Na^+})_{\text{sample}} \quad (4)$$

$$\text{Crustal fraction \%} = 100(C_x/C_{Ca^{2+}})_{\text{crustal}} / (C_x/C_{Ca^{2+}})_{\text{sample}} \quad (5)$$

2.2.8. Scavenging ratio

Scavenging ratios (W , dimensionless) were calculated according to Eq. 6 (Cheng and Zhang, 2017; He and Balasubramanian, 2008; Kasper-Giebl et al., 1999).

$$W = \frac{C_{\text{rain}}}{C_{\text{air}}} \times \frac{\rho_{\text{air}}}{\rho_w} \quad (6)$$

where, C_{rain} is the concentration, in $mg\ L^{-1}$, of each studied species in rainwater samples, and C_{air} is the concentration in $\mu g\ m^{-3}$, of the same species in the aerosol samples during the precipitation event. ρ_{air} and ρ_w are the densities of air ($1.290\ kg\ m^{-3}$) and water ($10^6\ mg\ L^{-1}$), respectively, at $20\ ^\circ C$ and $1\ atm$.

Following Blanco-Alegre et al. (2019); Cugerone et al. (2018), for the determination of W , the following considerations were taken into account:

- Only events in which the rainfall duration covered more than 15% of the 24 hours of sampling were considered (corresponding to an approximate period of half the mean duration of rain events).
- Rain events with a variation in wind speed greater than $2\ m\ s^{-1}$ were excluded from the sample.
- Due to aerosol samples were collected at 24-h intervals, it is assumed that the rainwater samples are representative of this sampling period.

2.2.9. Removal coefficients

Removal coefficients (ΔC_{rel}) were calculated as follows:

$$\Delta C_{\text{rel}} = \frac{\Delta C}{C_1} \times 100 = \frac{C_2 - C_1}{C_1} \times 100 \quad (7)$$

Where C_2 and C_1 are the concentration of the studied species after and before the precipitation event, respectively. Consequently, a negative ΔC_{rel} indicates effective scavenging.

Besides the considerations above mentioned for W determination, ΔC_{rel} was calculated as follows:

- Two types of precipitation events were considered: i) a “24-h event”, when the precipitation period covered more than 15% of the 24 hours of sampling and ii) a “full event”, taking the precipitation event as the consecutive rain days, and considering that the event ended when there was a minimum of 48 hours without precipitation after collection of the last rainwater sample.
- Aerosol concentrations before and after the precipitation event were obtained as a mean value, calculated from the concentrations 2 days before and 2 days after the event, respectively.

3. Results

3.1. Characterization of precipitation

During the sampling period, a total of 485 mm of precipitation, distributed in 118 days, was registered in León. This value is very close to the annual average precipitation, reported in León by the AEMET of 515 mm. April was the month with more precipitation days (18 days) and more accumulated precipitation (112.4 mm), followed by February and May (Fig. 2a). Besides, July, August and September were the months with less rain days. The lowest accumulated precipitation of the entire campaign (3.7 mm) was registered in July.

The mean precipitation intensity, taking into account the individual precipitation events, was $0.8\ mm\ h^{-1}$ in both spring and autumn, $1.7\ mm\ h^{-1}$ in summer and $0.7\ mm\ h^{-1}$ in winter. The longest precipitation episodes were recorded in spring, with a mean duration of 7 ± 5 days, and a maximum duration of 15 days, between 09 and 24 April 2016, although it only rained during 35% of the time period.

The most frequent weather type during the rainy days was the cyclonic type (C) with 21 days (19% of the total), followed by westerly types SW and W, both with 10 days (9% each of the total) (Fig. 2b). The weather types with more accumulated precipitation were: cyclonic (C) with 149 mm, westerly (W) with 68 mm and northwesterly cyclonic (CNW) with 62 mm. Regarding the average daily precipitation volume, the type CNW showed the highest value with $15.6\ mm\ day^{-1}$, followed by C with $7.1\ mm\ day^{-1}$ and W with $6.8\ mm\ day^{-1}$.

3.2. Aerosol chemical composition

During the sampling campaign, carbonaceous constituents (OC + EC), represented the highest PM_{10} mass fraction in all seasons, with an average annual percentage of $13 \pm 3\%$. Winter showed the highest carbonaceous fraction with a mean OC and EC concentrations of $2.7 \pm 1.5\ \mu g\ m^{-3}$ and $0.9 \pm 0.5\ \mu g\ m^{-3}$, respectively, while spring showed the lowest concentrations with 1.9 ± 1.0 and $0.7 \pm 0.3\ \mu g\ m^{-3}$, respectively. The elements related to the mineral fraction showed the highest concentrations in summer with 0.9 ± 0.7 , 0.3 ± 0.2 , 0.4 ± 0.2 and $0.4 \pm 0.4\ \mu g\ m^{-3}$ of Si, Fe, Ca and Al, respectively, probably due to the high incidence of Saharan dust intrusions on the Peninsula during this season. Moreover, the lowest concentrations of these elements were recorded in spring (0.3 ± 0.3 , 0.14 ± 0.08 , 0.16 ± 0.11 , $0.13 \pm 0.11\ \mu g\ m^{-3}$, respectively). In addition, Na and Cl, species related to sea salt aerosols, showed the highest concentrations in winter and the lowest in summer, with average values between 0.17 and $0.3\ \mu g\ m^{-3}$ for Na and between 0.07 and $0.5\ \mu g\ m^{-3}$ for Cl.

The highest sulfate values were observed in summer ($1.6 \pm 0.9\ \mu g\ m^{-3}$), mainly due to SO_2 oxidation under high insolation conditions (Galindo et al., 2008; Seinfeld and Pandis, 2016). Ammonium concentration in PM_{10} were similar in all seasons, with mean values of $0.5 \pm 0.3\ \mu g\ m^{-3}$ in summer, $0.6 \pm 0.5\ \mu g\ m^{-3}$ in autumn and spring and of $0.7 \pm 0.8\ \mu g\ m^{-3}$ in winter. Furthermore, the highest nitrate concentrations were recorded in winter ($1.3 \pm 1.5\ \mu g\ m^{-3}$), produced by the thermal stability of ammonium nitrate (Querol et al., 2004). More information and a discussion on the chemical composition of aerosols during this sampling campaign can be found in Oduber et al. (2021).

3.3. Rainwater chemical composition

3.3.1. Inorganic ions

During the sampling period, 74 rain samples, distributed in 31 precipitation events, were analyzed (Table 2). The season with more samples was winter, with 25 rainwater samples (in 23 precipitation

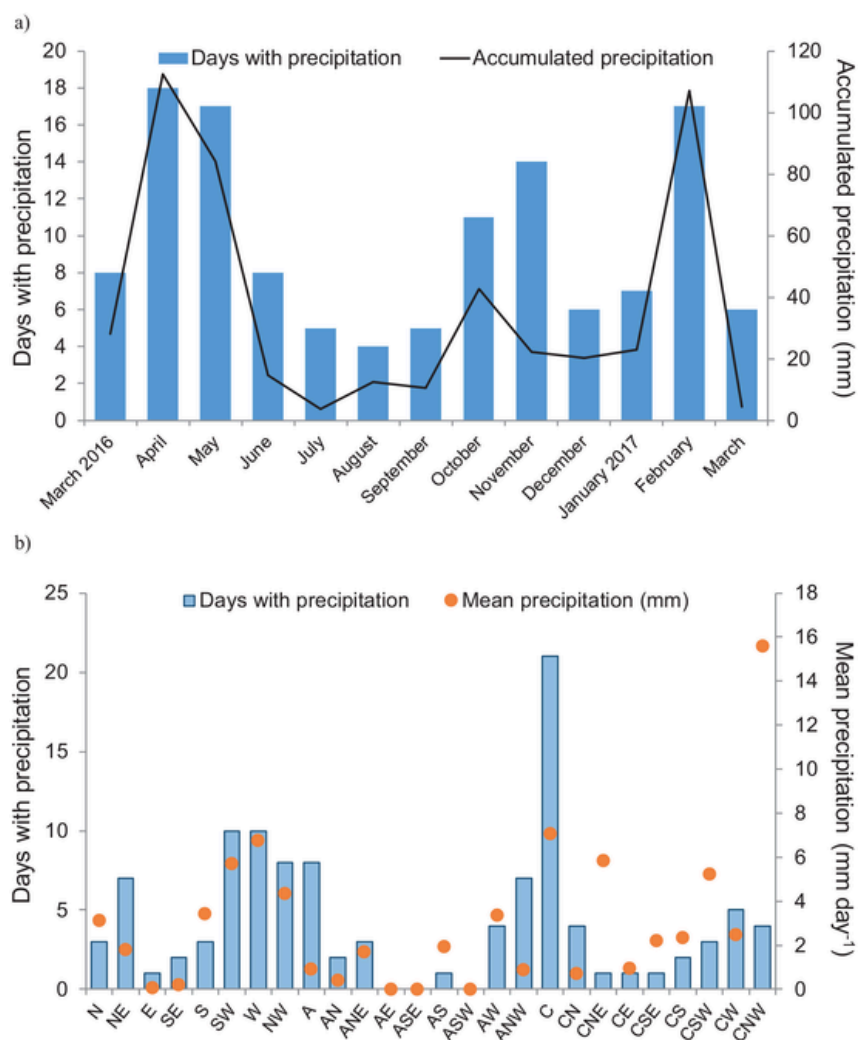


Fig. 2. a) Monthly evolution of days with precipitation and accumulated precipitation and b) days with precipitation and mean precipitation for each of the Circulation Weather Types.

events), although the season with more volume collected was spring. The season with less rainwater samples was summer, with 6.

The inorganic content of rainwater (Table 2) reveals a predominance of NH_4^+ , followed by SO_4^{2-} and NO_3^- . The statistical correlation between SO_4^{2-} , NO_3^- and NH_4^+ ($r > 0.9$, $p < 0.01$) and the source contribution indicate that nitrate and sulfate have a common origin, mainly anthropogenic (92.3 and 99.8%, respectively, Table S1). These elements, related to secondary aerosol showed their highest concentrations during the AN, CN and NE weather types (above $30 \mu\text{eq L}^{-1}$ for SO_4^{2-} , $48 \mu\text{eq L}^{-1}$ for NO_3^- and $70 \mu\text{eq L}^{-1}$ for NH_4^+), all of them with a northern flow component.

The highest VWM Na^+ and Cl^- concentrations were reached in winter, with 11.72 ± 0.11 and $14.61 \pm 0.12 \mu\text{eq L}^{-1}$, respectively (Table 2). Both the enrichment factor of 1.2 (Table S1) and the significant correlation between these two ions ($r = 0.91$, $p < 0.01$), reflect the common marine origin. The highest VWM values of these sea-salt related elements, were recorded during the CS, CN, AN and SW weather types (Fig. 3a and 3b), reaching concentrations between 25 and $43 \mu\text{eq L}^{-1}$ for Na^+ and between 27 and $58 \mu\text{eq L}^{-1}$ for Cl^- .

High K^+ , Ca^{2+} and Mg^{2+} concentrations were recorded in summer (5.21 , 35 and $7.6 \mu\text{eq L}^{-1}$), while the lowest concentrations were recorded in spring (Table 2). The highest volumetric concentrations of crustal-related elements, Ca^{2+} and Mg^{2+} , were observed in AN, CS and NE weather types, with VWM values ranging between 17 and $101 \mu\text{eq L}^{-1}$ for Ca^{2+} and between 12 and $16 \mu\text{eq L}^{-1}$ for Mg^{2+} . Moreover, the

lowest VWM values were recorded mainly in the hybrid cyclonic types CNE and CSW (Fig. 3b).

3.3.2. Carbonaceous fraction

The organic carbonaceous fraction can be scavenged by wet deposition in two forms, soluble (DOC) and insoluble (WIOC) fractions. The contribution from DOC to the total organic fraction ranged between 71% and 82%, with the lowest contribution obtained in summer and the highest in winter. However, in summer and autumn the DOC values are higher (Table 2). DOC values are higher for NE, CE and CNE weather types (Fig. 3c), reaching concentrations up to 8 mg L^{-1} .

There was a significant correlation between WIEC and WIOC during winter and spring and the highest WIOC concentrations were recorded for CW and AN weather types, while the highest WIEC were observed for CW, CN and AN weather types (Fig. 3c).

3.4. Acidic contribution

The individual pH values of rainwater ranged between 4.2 and 7.2 (Fig. 4a). The VWM pH of the entire campaign was 5.87 ± 0.02 , while the mean annual conductivity was $27.0 \pm 0.2 \mu\text{S cm}^{-1}$, reflecting the low influence on precipitation of emissions from large industries and other local sources. The lowest conductivity ($2.77 \mu\text{S cm}^{-1}$, in 103 mL) and highest pH value (7.20, in 38 mL) were observed in May 2016 and

Table 2

Annual and seasonal volume-weighted mean (VWM) ion concentrations, dissolved organic carbon (DOC), water insoluble organic and elemental carbon (WIOC and WIEC, respectively) in rainwater.

	Annual	Winter	Spring	Summer	Autumn
Number of 24-h event types	31	8	9	4	10
Total precipitation (mm)	363	130	130	25	78
Number of rainwater samples collected	74	25	23	6	20
Volume collected (L)	16.64	5.63	6.68	0.48	3.85
VWM ($\mu\text{eq L}^{-1}$)					
Na ⁺	6.64 ± 0.07	11.72 ± 0.11	3.35 ± 0.08	5.3 ± 0.3	5.2 ± 0.2
NH ₄ ⁺	21.5 ± 0.2	14.7 ± 0.2	24.5 ± 0.2	40 ± 2	20.7 ± 0.3
Mg ²⁺	3.19 ± 0.02	3.97 ± 0.03	2.09 ± 0.02	7.6 ± 0.2	2.50 ± 0.05
K ⁺	3.37 ± 0.01	3.02 ± 0.02	2.92 ± 0.02	5.21 ± 0.04	4.03 ± 0.03
Ca ²⁺	5.92 ± 0.11	8.80 ± 0.10	8.09 ± 0.10	35 ± 2	5.02 ± 0.08
Cl ⁻	9.43 ± 0.08	14.61 ± 0.12	6.67 ± 0.11	9.2 ± 0.3	6.6 ± 0.2
SO ₄ ²⁻	13.59 ± 0.08	14.62 ± 0.12	12.33 ± 0.10	20.2 ± 0.9	12.11 ± 0.15
NO ₃ ⁻	13.18 ± 0.09	10.52 ± 0.09	13.07 ± 0.11	27.0 ± 1.3	12.81 ± 0.11
VWM (mg L⁻¹)					
DOC	1.554 ± 0.014	1.520 ± 0.011	0.685 ± 0.004	2.92 ± 0.15	2.57 ± 0.05
WIOC	0.234 ± 0.002	0.173 ± 0.002	0.225 ± 0.004	0.83 ± 0.02	0.1522 ± 0.0015
WIEC	0.0180 ± 0.0001	0.0157 ± 0.0002	0.0211 ± 0.0003	0.0192 ± 0.0003	0.0158 ± 0.0002

February 2017 (Fig. 4b), respectively, after several days of continuous rain. The highest conductivity (164.90 $\mu\text{S cm}^{-1}$, in 27 mL) and lowest pH (4.23, in 304 mL) were registered during forest fire events that took place in Portugal between June and August 2016. Emissions from biomass burning generate, on the one hand, an acidification of rainwater, due to the presence of acidic organic species (dicarboxylic acids and related compounds, such as the glycolic, lactic, hydroxybutyric and levulinic acids) and, on the other hand, an increase in conductivity caused by the increase in the concentration of inorganic ions soluble in water, such as SO₄²⁻, NO₃⁻ and NH₄⁺ (Oduber et al., 2020).

The highest neutralization factor was obtained by NH₄⁺ with 0.8 ± 0.5 , while the lowest NF was found for Mg²⁺ with 0.09 ± 0.09 (Table S2).

3.5. Scavenging ratios

The scavenging ratios (*W*) provide valuable information on the relationship between the concentration of the pollutants in rainwater and their concentrations in air. The scavenging ratios were higher in summer than in other seasons, except for Na⁺, K⁺, SO₄²⁻ and EC (Table 3). Ions related to marine and crustal sources (Na⁺, Mg²⁺, Cl⁻ and Ca²⁺) show high *W* values, indicating that they could be scavenged more efficiently than ions mainly bound to the fine fraction, such as the anthropogenic ions (NO₃⁻, SO₄²⁻ and NH₄⁺) and K⁺, which showed lower *W* values. However, NH₄⁺ exhibited one of the highest scavenging ratios in spring and summer.

3.6. Removal coefficients

The removal coefficient (ΔC_{rel}) allow us to infer information about the removal mechanism in the air, through the evolution of the concentration of pollutants before and after a precipitation event. Principal component analysis (PCA) was performed by applying a matrix of Varimax rotated components to the studied species in the aerosol samples. Three main groups were extracted, explaining more than 88.5% of the accumulated variance (Tables S4 and S5), according to their common origin: a) Al, Si, Ca, Ti, Fe, Mg, Mn and K as crustal elements (explaining more than 53% of the variance); b) NH₄⁺, SO₄²⁻, NO₃⁻ as secondary aerosol (18% of the variance) and c) Na and Cl as marine elements (16% of the variance). Episodes of high aerosol emissions (dust intrusion, biomass combustion and sulfate episodes) causing an extreme increase in concentrations during the precipitation event were excluded from the database for the calculation of removal coefficients, since they are not representative for this study.

The results show that, in general, the removal coefficients of almost all studied species present negative values (Fig. 5), indicating that precipitation helps to reduce the concentrations of all these species in the atmosphere. When comparing the monthly removal coefficient of the 24 h events with those of the full events (Fig. 5a and 5b), it is observed that scavenging is more efficient when the precipitation event is longer, increasing the ΔC_{rel} by 82 %, on average.

The effect of the precipitation intensity and duration on the removal coefficient is shown in Fig. 6. In general, intensities between 0.5 and 0.8 mm h⁻¹ showed an increase in the removal coefficient for long time periods (> 20 hours of rain). Intensities higher than 0.9 mm h⁻¹ show maxima ΔC at short periods of time (between 4 and 6 hours).

3.7. Linear predictive models for rain scavenging and for chemical properties of rainwater

Linear models have been built from the data obtained for each studied species in each event. The statistically significant models for the prediction of rainwater chemical characteristic were: a) concentrations in rainwater of WIOC, DOC, WIEC, SO₄²⁻ and NO₃⁻, b) mass in rainwater of Ca²⁺, SO₄²⁻, c) scavenging ratios (*W*) of NO₃⁻, and d) removal coefficients (ΔC) during 24h events and ΔC during full events for PM₁₀, OC, EC, crustal, marine and secondary aerosol.

Previously, the Pearson correlations were calculated between rainwater concentrations, *W* and ΔC with the following independent variables:

- 3- Chemical aerosol properties: the concentration in air of each species before precipitation (*C*₁).
- 3- Physical parameters of precipitation: event duration, time with precipitation during the daily sampling period of aerosol (*t*), accumulated precipitation (*Prec.*), mean rainfall intensity (*Intensity*), mean raindrop size (*D*_{size}), sum of volume swept by falling drops (*V*_{swept}), total number of drops (*N*_{drops}). Besides, the time without rain between two precipitation events (*t*_{before}) has been included.

With these parameters, a model has been built from a random sample that includes 75% of the total data set. This model has been run to the remaining 25% and then, a Kolmogorov-Smirnov statistical test has been applied to check the goodness of fit. This process has been repeated five times.

All chemical and physical variables were checked for the building of the model. Nevertheless, Table 4 only shows the dependent and independent variables and the statistically significant coefficients (*p* < 0.05) used to construct the multi-linear models. The significant values

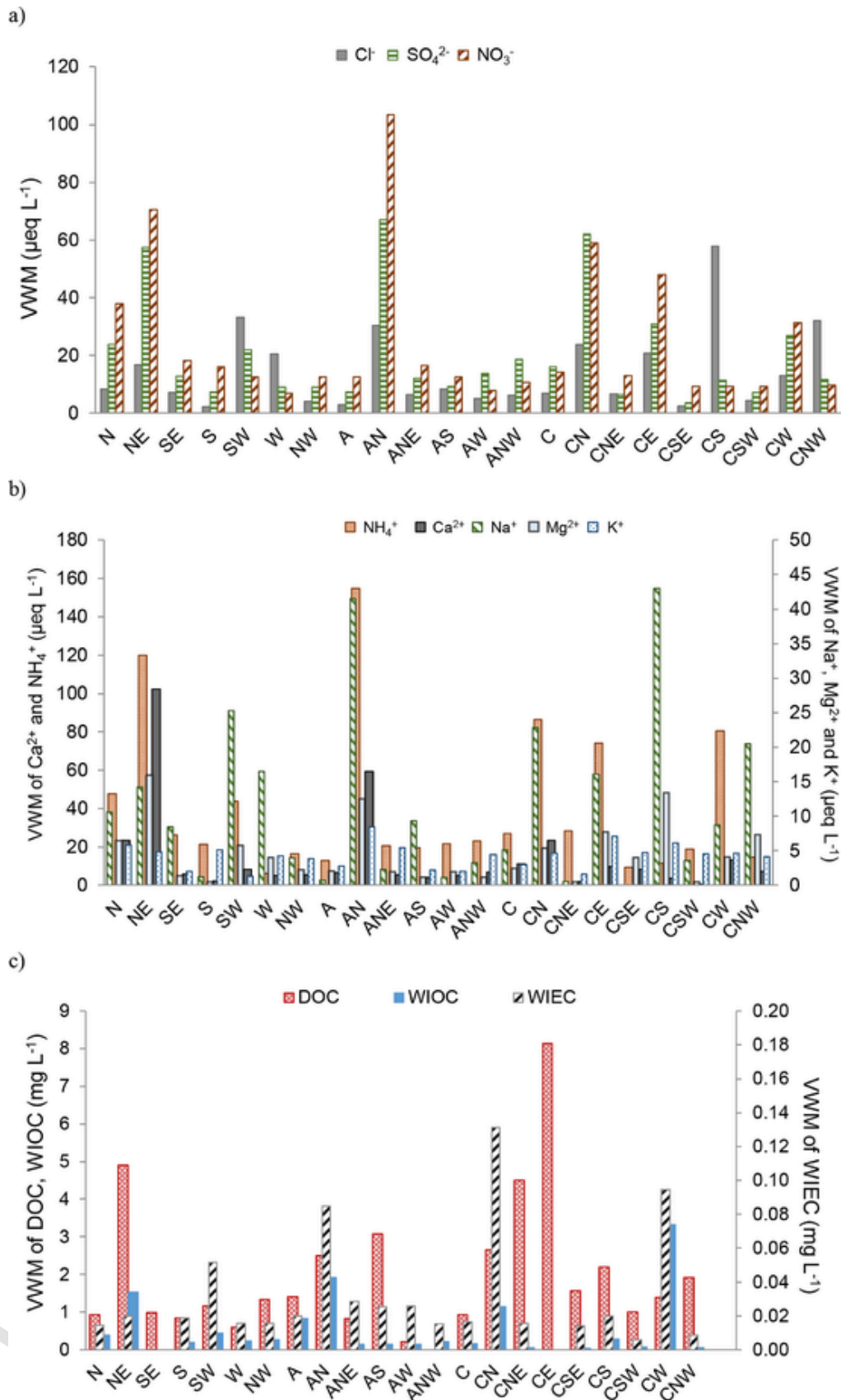


Fig. 3. Volume-Weighted Mean (VWM) for the different categories of Circulation Weather Types (CWT) for a) inorganic anions, b) inorganic cations and c) the carbonaceous fraction (DOC, WIOC, WIEC).

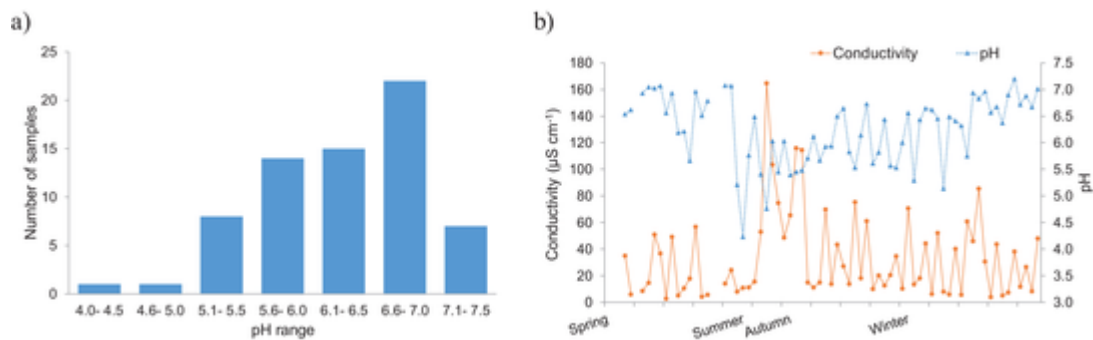


Fig. 4. a) Frequency distribution of pH and b) daily evolution of pH and conductivity of rainwater samples.

Table 3

Seasonal scavenging ratios (W , dimensionless) for each analyzed species and mean seasonal precipitation intensity.

Season	Intensity (mm h ⁻¹)	$W (\times 10^3)$									
		Na ⁺	NH ₄ ⁺	Mg ²⁺	K ⁺	Ca ²⁺	Cl ⁻	SO ₄ ²⁻	NO ₃ ⁻	EC	DOC + WIOC
Winter	0.7 ± 0.9	178.9	108.3	183.1	31.6	106.2	60.0	51.5	24.6	0.034	1.6
Spring	0.8 ± 0.6	47.1	228.0	106.9	67.4	88.3	116.2	46.8	46.5	0.136	1.4
Summer	1.7 ± 1.5	88.3	290.9	823.4	59.3	231.7	1061.9	35.9	157.8	0.013	5.7
Autumn	0.8 ± 1.7	109.9	64.7	126.7	59.3	110.7	45.0	30.5	26.4	0.049	2.3

obtained show that the measured and predicted data are related and, consequently, the model created can be applicable.

The multi-linear models shown in Table 4, were constructed as:

$$y_j = \sum \alpha_{ij} X_{ij} + \beta_j \quad (8)$$

where subscript $j = 1$ to 18 refers to the dependent variables (Table 4): rainwater concentrations, W and ΔC . For each dependent variable y_j that we need to estimate, the model gives the coefficients α_{ij} of each independent variable i ($i = 1$ to 6) and the intercept β_j .

4. Discussion

4.1. Rainwater chemical composition and weather types

The predominance of NH₄⁺, SO₄²⁻ and NO₃⁻ on rainwater and the high levels of these secondary species during the AN, CN and NE weather types, may be due to the presence of two major companies, a thermal power plant and a cement factory about 30 km north of León (Fig. 1). A PMF source apportionment studied in a previous paper (Oduber et al., 2021) showed the main natural and anthropogenic sources in León during the same study period. This study evidenced the influence of the emissions from the cement factory and the thermal power plant in León city. Furthermore, data from a local air quality station in La Robla (<http://servicios.jcyl.es/esco/cargarFrmDatosHistoricos.action>) show high SO₂ concentrations when compared with those from León city. This can be due to the presence of both factories. In addition, from the point of view of medium and long-range transport of pollutants, northeast is the direction where the air masses from industrial areas in Spain and Europe come from.

The high Ca²⁺ and Mg²⁺ concentrations in summer reflected the contribution from dust intrusion events which arrived at the Peninsula during warmer months, confirmed by the enrichment factor result (Table S1). Furthermore, the highest potassium concentration observed also in summer is probably due to the frequent forest fires and African dust events that occur in the Iberian Peninsula that could rise the K⁺ values (Vicente et al., 2013). The weather types associated with the highest volumetric concentrations of Ca²⁺ and Mg²⁺ (AN, CS and NE),

were previously related to a high contribution of mineral aerosols and aged sea salt, enriched with crustal-related elements during transport to León (Oduber et al., 2021). Moreover, the lowest VWM values observed for all the species can be due to the significant dispersion of the contaminants in the cyclonic circulations and large periods of continuous precipitation.

Regarding the carbonaceous fraction, less than 3 km NE of the city of León there is a large mass of plants (Fig. 1), which contributes a large amount of biogenic material and may be responsible for the increase in concentrations of dissolved organic carbon (Oduber et al., 2019b) observed for NE, CE and CNE weather types. Moreover, the weather types CW and AN exhibited a high concentration of WIOC and WIEC because the air masses coming from the north and west of León probably incorporate carbonaceous species from anthropogenic sources during their trajectory to the city. Furthermore, the weather type CN showed a high influence of road traffic emissions (Oduber et al., 2021) contributing to WIEC concentrations. The significant correlation between WIEC and WIOC during winter and spring ($r > 0.7$, $p < 0.01$) may indicate a common origin (traffic and fossil fuel primary emissions) (Favez et al., 2008; Theodosi et al., 2010).

In addition, there is a significant correlation between DOC and the main crustal elements in summer and spring ($r > 0.5$, $p < 0.05$). In these seasons, the air masses coming mainly from the south, travel through large areas of forest until they reach León; therefore, the concentration of dissolved organic carbon could be partly related to the transport of biogenic material from the south of the Iberia Peninsula. Thus, the correlation observed between DOC and crustal elements is probably due to the transport of this material together with the biogenic one (Oduber et al., 2020). Furthermore, the highest photochemical activity during these seasons could also contribute to the oxidation of volatile organic compounds (VOCs) into soluble organic particles. Between summer and spring there is also a high incidence of wildfires in the Iberian Peninsula (Alonso-Blanco et al., 2012; Alves et al., 2011; Vicente et al., 2013, 2012), that can emit large amount of water-soluble organic compounds (Alves et al., 2011), causing an increase in DOC concentrations.

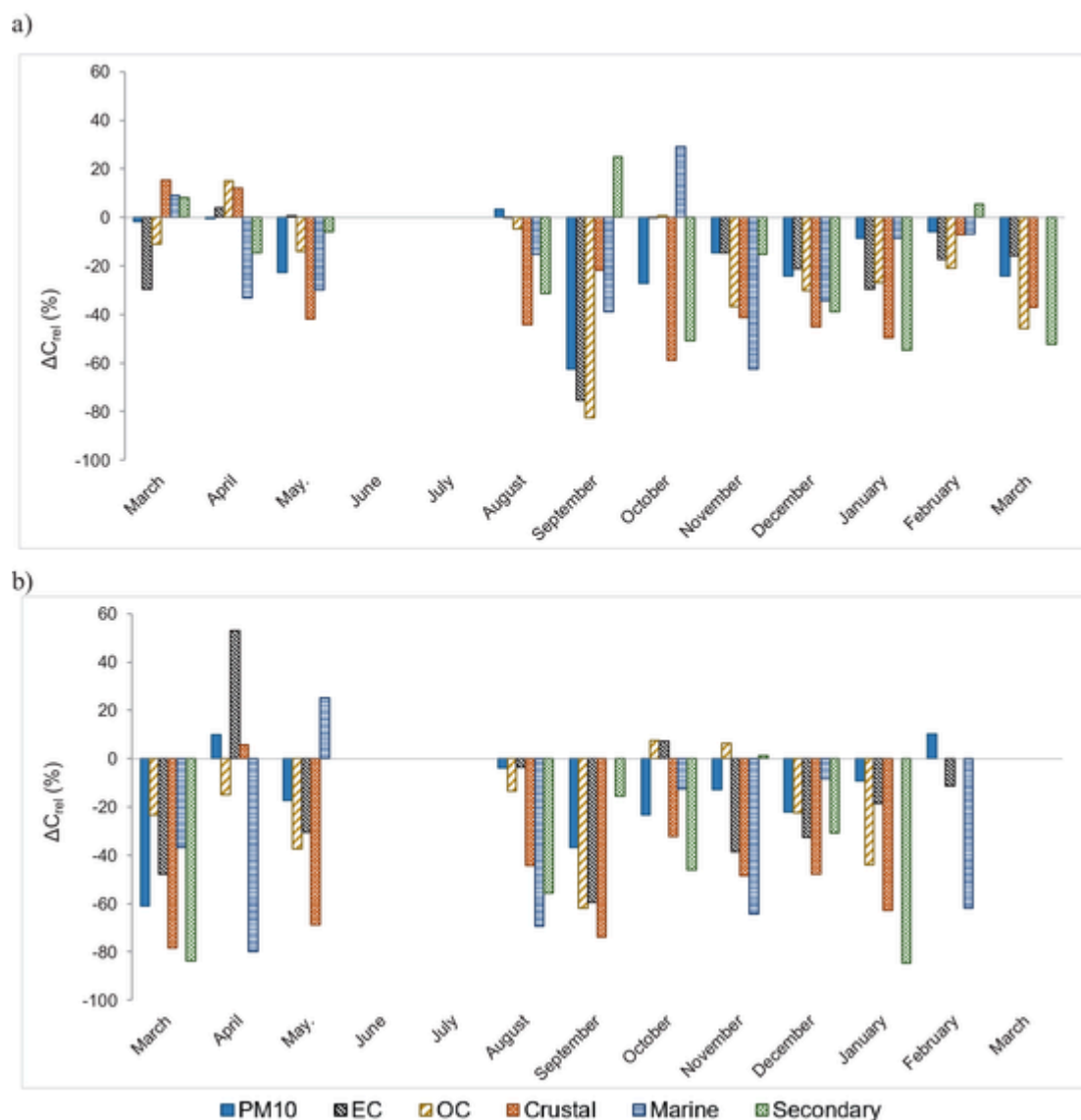


Fig. 5. Monthly evolution of removal coefficients (ΔC_{rel}) of particulate matter (PM₁₀), carbon fractions (EC and OC), crustal elements (Al, Si, Ca, Ti, Fe, Mg, Mn and K), marine elements (Na and Cl), secondary aerosol (NH₄⁺, SO₄²⁻, NO₃), for a) 24-h rainwater samples and b) full events of precipitation.

In autumn and winter, the domestic heating systems constitute an important source of DOC (Siudek et al., 2015). Although in winter the concentration of OC in PM₁₀ is higher than in autumn, the concentration of DOC is lower. It is probably due to the larger volume of total precipitation recorded in winter (Table 2). Furthermore, in autumn, DOC concentrations could also be affected by the presence of forest fires and by agricultural stubble burning, not common in winter.

4.2. Acidic contribution

The Kruskal-Wallis test, applied to the pH values obtained for the individual rainwater samples, shows significant differences between pH values of spring rainwater samples and those of summer and autumn. Winter and spring are rainy seasons in León, which helps to clean the atmosphere. Consequently, an increase in the pH and a decrease in the conductivity of the rainwater can be observed when compared to other seasons. A reduction of the conductivity values due to the abundant rainfall was also observed by Zhang et al. (2007) in rainwater samples from southern China, indicating the dilution effect on the atmospheric pollution.

The results obtained for the neutralization factor suggest that the crustal components neutralized a small fraction of the available acid in the precipitation and that ammonia plays an important role in the neutralization of the rainwater mainly in winter. Ca²⁺ shows statistically significant differences between the NF values of summer and the rest of the seasons, confirming the neutralizing effect of this crustal component when the dust contribution is greater. The high NF of Na in winter (0.7 ± 0.8) could partly justify the high pH values observed in this season.

4.3. Scavenging ratios and removal coefficients

Table 3 shows that in general, scavenging ratios were higher in summer than in other seasons, except for Na⁺, K⁺, SO₄²⁻ and EC. In León, convective phenomena are frequent in summer, which generally cause short and intense precipitation events (Fernández-Raga et al., 2017). Kulshrestha et al. (2003, 2009) studied the relation between the aerosol size and duration of precipitation in below-scavenging processes, reporting that scavenging ratios increase with the increase of the precipitation intensity for species present in fine particles, such as

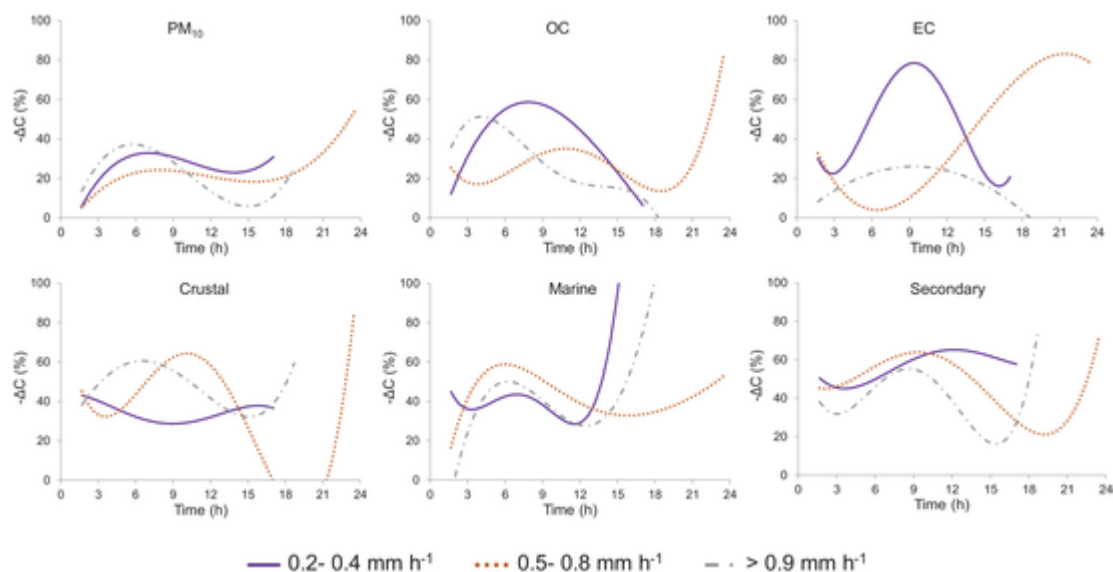


Fig. 6. Evolution of the removal coefficient with the duration of the daily precipitation event as a function of the rain intensity and for PM_{10} , carbonaceous fraction (OC and EC), crustal, marine and secondary aerosols.

NH_4^+ , K^+ and NO_3^- . Moreover, the soil-derived coarse particles are also effectively scavenged due to the inertial impaction by raindrops through the rain columns. The scavenging ratio also depends on the particle sizes. As in this work, Encinas et al. (2004); Jaffrezo and Colin (1988), reported high W values for ions related to marine and crustal sources (Na^+ , Mg^{2+} , Cl^- and Ca^{2+}), and lower W values for ions related to fine particles. Therefore, the scavenging process is more efficient in coarse particles. However, the opposite result observed for NH_4^+ in spring and summer, could be related to other processes. The composition of the rainwater is determined by the scavenging process of both gases and particles, thus, the scavenging ratios can be overestimated for some species such as Cl^- , NO_3^- , SO_4^{2-} and NH_4^+ , due to the incorporation to the rain droplets of the gases HNO_3 , HCl , SO_2 and NH_3 , especially in spring and summer, when the formation of secondary aerosols is favored by the photochemical reactions. Kasper-Giebl et al. (1999) report that NO_3^- values in rainwater are predominantly due to gas-phase scavenging of HNO_3 (88-96%), while NH_4^+ in rainwater is formed between 49 and 79% by particulate NH_4^+ .

Regarding removal coefficients (Fig. 5), the negative values observed for almost all studied species, indicate that precipitation helps to clean the atmosphere. The increase in removal coefficients for full events compared to 24-hour events shows that the removal process is more efficient when the precipitation event is longer. Olszowski (2014) reported that rainfalls with six hours of duration are 3.5 times more effective than similar intensity rainfalls with half an hour of duration in removing PM_{10} .

The effect of the intensity and duration of precipitation on the removal coefficient (Fig. 6), indicates that the scavenging process is more efficient with long and continuous periods of precipitation at intensities between 0.5 and 0.8 $mm\ h^{-1}$, while at high intensities the scavenging process is efficient at short periods of time. Olszowski (2014) observed that rains with intensities greater than 4 $mm\ h^{-1}$ are approximately 35% more effective in removing PM from the air than precipitations with intensities lower than 0.5 $mm\ h^{-1}$, suggesting that PM_{10} concentrations increase much faster after a light rain event. Similar results were also reported by Castro et al. (2010) in a study carried out in León, Spain, in spring 2005, when it was observed that with intensities over 3.2 $mm\ h^{-1}$, there was an intense washout and the number of both small and large particles decreased significantly. However, low rain intensities (< 0.5 $mm\ h^{-1}$) showed high removal coefficients in a period between 7 and 9 hours, except for crustal-related ele-

ments, and an increase of ΔC in long periods for the elements related to secondary aerosols. These results, as well as those reported by Kulshrestha et al. (2009), suggest that short-duration and high-intensity rain events effectively remove coarse mode particles, such as particles related to crustal and marine sources, probably by a process of below-cloud scavenging, while rain of low intensity, but with longer duration, is more effective in removing fine particles.

4.4. Linear predictive models

The linear models for predicting the rain scavenging and for chemical properties of rainwater were constructed as explained in Section 3.7. They can be seen in Table 4 showing that:

- 3- The amount of DOC and water-soluble ions in rain samples, Ca^{2+} , SO_4^{2-} , NO_3^- , increases with the volume swept by the falling drops, probably due to the high solubility in water of these compounds. In other words, a high volume of precipitation (or a large number of drops) favors the elimination of these species.
- 3- A negative dependence between V_{swept} and WIEC was observed, while the WIOC is dependent of the raindrop diameter and the time between two precipitation events. Scavenging of insoluble species can be more affected by the inertial impact of the raindrops through the columns of rain. This behavior was also described by Blanco-Alegre et al. (2019), who deduced a multi-linear model to estimate the black carbon scavenging by rain.
- 3- In general, the removal coefficient and the decrease in the concentration of PM_{10} , OC, EC, crustal, marine and secondary related aerosols after a precipitation event is affected by the concentration of each species before the event. The negative coefficient in all cases shows that the higher the concentration before the precipitation event, the more efficient the elimination process.
- 3- The ΔC of the 24-hour events showed positive coefficients for the time elapsed between two consecutive precipitation events, while the ΔC for full events show a negative dependence with the percentage of time with precipitation during the sampling period. Therefore, the scavenging of pollutants is more efficient with prolonged and continuous precipitation events. These results are consistent with those observed by Castro et al. (2010) in the study carried out in León, Spain, in the spring of 2005. They observed that with rain intensities lower than 0.6 $mm\ h^{-1}$, the time it took for the num-

Table 4

Coefficients of multi-linear regression models for rainwater concentration of each species (C_{rain}), scavenging ratios (W) and removal coefficients (ΔC).

y_j	β_j (mg L^{-1})	Chemical aerosol properties	Physical precipitation parameters				R^2
		C_1 ($\mu\text{g m}^{-3}$)	t (%)	Intensity (mm h^{-1})	D_{size} (mm)	V_{swept} ($\text{mm}^3 \text{m}^{-3}$)	t_{before} (min)
		α_{1j}	α_{2j}	α_{3j}	α_{4j}	α_{5j}	α_{6j}
		($\text{m}^3 \text{mg} \mu\text{g}^{-1} \text{L}^{-1}$)	($\text{mg L}^{-1} \%^{-1}$)	($\text{mg h L}^{-1} \text{mm}^{-1}$)	($\text{mg L}^{-1} \text{mm}^{-1}$)	($\text{mg m}^{-3} \text{L}^{-1} \text{mm}^{-3}$)	($\text{mg L}^{-1} \text{min}^{-1}$)
C_{rain} (mg L^{-1})							
WIOC	-1.40				2.82×10^{-5}		4.71
DOC	1.51						2.88×10^{-4}
WIEC	0.06					-1.30×10^{-9}	0.29
SO_4^{2-}	2.44			3.22			0.30
NO_3^-	3.79					1.30×10^{-7}	-0.00019
	β_j (mg)	α_{1j} ($\text{m}^3 \text{mg} \mu\text{g}^{-1}$)	α_{2j} ($\text{mg} \%^{-1}$)	α_{3j} (mg h mm^{-1})	α_{4j} (mg mm^{-1})	α_{5j} ($\text{mg m}^{-3} \text{mm}^{-3}$)	α_{6j} (mg min^{-1})
Mass in rainwater (mg)							
Ca^{2+}	-2.20					2.27×10^{-7}	0.37
SO_4^{2-}	-1.73					1.81×10^{-7}	0.41
	β_j	α_{1j} ($\text{m}^3 \mu\text{g}^{-1}$)	α_{2j} ($\%^{-1}$)	α_{3j} (h mm^{-1})	α_{4j} (mm^{-1})	α_{5j} ($\text{m}^{-3} \text{mm}^{-3}$)	α_{6j} (min^{-1})
W (dimensionless)							
NO_3^-	4.99×10^4	-2.00×10^4					4.99
	β_j ($\mu\text{g m}^{-3}$)	α_{1j}	α_{2j} ($\mu\text{g m}^{-3} \%^{-1}$)	α_{3j} ($\mu\text{g h m}^{-3} \text{mm}^{-1}$)	α_{4j} ($\mu\text{g m}^{-3} \text{mm}^{-1}$)	α_{5j} ($\mu\text{g m}^{-3} \text{m}^{-3} \text{mm}^{-3}$)	α_{6j} ($\mu\text{g m}^{-3} \text{min}^{-1}$)
ΔC (24-h event) ($\mu\text{g m}^{-3}$)							
PM_{10}	7.79	-0.53					0.50
OC	1.12	-0.85					4.50×10^{-5}
EC	0.55	-0.99					7.50×10^{-6}
Crustal	0.09	-0.90		0.13		-5.94×10^{-9}	5.40×10^{-6}
Marine	0.15	-0.57					0.29
Secondary	0.35	-0.88					3.81×10^{-5}
	β_j ($\mu\text{g m}^{-3}$)	α_{1j}	α_{2j} ($\mu\text{g m}^{-3} \%^{-1}$)	α_{3j} ($\mu\text{g h m}^{-3} \text{mm}^{-1}$)	α_{4j} ($\mu\text{g m}^{-3} \text{mm}^{-1}$)	α_{5j} ($\mu\text{g m}^{-3} \text{m}^{-3} \text{mm}^{-3}$)	α_{6j} ($\mu\text{g m}^{-3} \text{min}^{-1}$)
ΔC (full event) ($\mu\text{g m}^{-3}$)							
PM_{10}	19.16		-0.77				0.56
OC	3.57	-0.54	-0.08				0.82
Crustal	0.27	-0.64	-0.007				0.73
Secondary	2.60	-1.02	-0.05				0.84

ber of particles to regain values similar to the initial number registered before the precipitation event was about 2 h.

- 3- The model for the scavenging ratio (W) was significant only for NO_3^- , depending on the time between two rain events and their concentration in the aerosol before the rain event. This is consistent with the inverse relationship of W and C_{air} (Eq. (6)).

It is important to realize that these models only depend on the physical properties of the rain and the chemical characteristics of the aerosol. As a consequence, they can probably be applied in any region, as they do not depend on regional conditions such as weather or local features.

5. Conclusions

A one-year sampling campaign was carried out between March 2016 and March 2017, in order to characterize the below cloud scavenging process and establish linear models showing the influence of the physical parameters of raindrops and the chemical properties of

aerosols on the removal of atmospheric pollutants. A total of 363 mm of precipitation were recorded during the entire sampling period, April being the month with more rain days and more accumulated rainwater and July the month with fewer days and less accumulated rainfall.

The chemistry of the rainwater sampled provided evidence on the contribution mainly from anthropogenic sources, through the high values of NH_4^+ , SO_4^{2-} and NO_3^- . In winter, the high values of Na^+ and Cl^- in the rainwater composition show the contribution from the sea. These species arrived in León with the air masses from the Atlantic and are related to CS, CN, AN and SW weather types. This source could also explain the high values of pH in the precipitation sampled in winter season. Moreover, summer precipitation is characterized by high concentrations of elements from crustal and anthropogenic sources, mainly related to air masses from North Africa and AN, CS and NE weather types. The mean pH and conductivity of the rainwater were 5.87 and $27.0 \mu\text{S cm}^{-1}$, respectively, indicating the low influence of large industries and other local anthropogenic sources in León. The carbonaceous fraction was dominated by DOC, showing the lowest values in summer and the highest in winter. In summer, the dissolved organic carbon

concentrations could be related to the transport of biogenic material from the south of the Iberian Peninsula, and secondary organic carbon production, while in winter they could be linked to traffic and fossil fuel primary emissions.

Scavenging ratios show that: i) the soil-derived coarse particles are effectively removed with the increase of the precipitation intensities; ii) for fine particles, this process is more effective with long and continuous rainfall; iii) for ammonium, they increase due to the incorporation of NH_4^+ in gas-phase to the drop. Regarding the removal coefficients, the increase observed for full events versus 24-hour events indicate that the removal process is more efficient when the precipitation event is longer. Rainfall intensity also affects the efficiency of the scavenging process. At low intensities the scavenging is favored by long and continuous rains, while at intensities above 0.9 mm h^{-1} , scavenging efficiency is favored when the rain duration is between 4 and 6 hours.

Linear models for the prediction of the chemical composition of rain-water, scavenging ratio and removal coefficients were constructed. The results showed that only the amount of the water-soluble ions in rainwater, Ca^{2+} , SO_4^{2-} , NO_3^- , increases with the volume swept by the drops, while the concentration of water insoluble organic and elemental carbon is affected by raindrop diameter and swept volume, respectively. The removal coefficients (ΔC) are affected by the air concentration of each species before precipitation, by the duration of the precipitation event and by the elapsed time between two events.

The results confirm the influence of physicochemical properties of the rain and the chemical properties of aerosols in the elimination of atmospheric pollutants.

This work represents a further step in the study of the mechanisms of elimination of air pollutants, proving that simple models can allow a first approach to the calculation of the efficiency of removal of pollutants by rain in a region, considering not only the chemical characteristics of the precipitation, but also its physical properties, which represent a scarce studied field.

6. Funding sources

This study was partially supported by the Spanish Ministry of Science, Innovation and Universities (Grant RTI2018-098189-B-I00), the AERORAIN project (Ministry of Economy and Competitiveness, Grant CGL2014-52556-R, co-financed with FEDER funds), the University of León (Programa Propio 2015/00054/001 and 2018/00203/001), the AEROHEALTH project (Ministry of Science and Innovation, Grant PID2019-106164RB-I00, co-financed with European FEDER funds) and the Junta de Castilla y León co-financed with European FEDER funds (Grant LE025P20). F. Oduber acknowledges the grant BES-2015-074473 from the Spanish Ministry of Economy and Competitiveness. C. Blanco-Alegre acknowledges the grant FPU16-05764 from the Spanish Ministry of Education, Culture and Sport.

7. Uncited references

Alves et al., 2015,

Declaration of Competing Interest

The authors declare that they have no known competing financial interests or personal relationships that could have appeared to influence the work reported in this paper.

Acknowledgments

This study was partially supported by the Spanish Ministry of Science, Innovation and Universities (Grant RTI2018-098189-B-I00), the AERORAIN project (Ministry of Economy and Competitiveness, Grant CGL2014-52556-R, co-financed with FEDER funds), the University of León (Programa Propio 2015/00054/001 and 2018/00203/001), the

AEROHEALTH project (Ministry of Science and Innovation, Grant PID2019-106164RB-I00, co-financed with European FEDER funds) and the Junta de Castilla y León co-financed with European FEDER funds (Grant LE025P20). F. Oduber acknowledges the grant BES-2015-074473 from the Spanish Ministry of Economy and Competitiveness. C. Blanco-Alegre acknowledges the grant FPU16-05764 from the Spanish Ministry of Education, Culture and Sport.

Supplementary materials

Supplementary material associated with this article can be found, in the online version, at doi:10.1016/j.watres.2020.116758.

References

- Alastuey, A., Querol, X., Chaves, A., Ruiz, C.R., Carratala, A., Lopez-Soler, A., 1999. Bulk deposition in a rural area located around a large coal-fired power station, northeast Spain. *Environ. Pollut.* 106, 359–367. doi:10.1016/S0269-7491(99)00103-7.
- Alonso-Blanco, E., Calvo, A.I., Fraile, R., Castro, A., 2012. The influence of wildfires on aerosol size distributions in rural areas. *Sci. World J.* 2012, 1–13. doi:10.1100/2012/735697.
- Alves, C.A., Lopes, D.J., Calvo, A.I., Evtyugina, M., Rocha, S., Nunes, T., 2015. Emissions from light-duty diesel and gasoline in-use vehicles measured on chassis dynamometer test cycles. *Aerosol Air Qual. Res.* 15, 99–116. doi:10.4209/aaqr.2014.01.0006.
- Alves, C.A., Vicente, A., Monteiro, C., Gonçalves, C., Evtyugina, M., Pio, C., 2011. Emission of trace gases and organic components in smoke particles from a wildfire in a mixed-evergreen forest in Portugal. *Sci. Total Environ.* 409, 1466–1475. doi:10.1016/j.scitotenv.2010.12.025.
- Bernstein, J.A., Alexis, N., Barnes, C., Bernstein, I.L., Nel, A., Peden, D., Diaz-Sanchez, D., Tarlo, S.M., Williams, P.B., Bernstein, J.A., 2004. Health effects of air pollution. *J. Allergy Clin. Immunol.* 114, 1116–1123. doi:10.1016/j.jaci.2004.08.030.
- Blanco-Alegre, C., Calvo, A.I., Coz, E., Castro, A., Oduber, F., Prévôt, A.S.H., Močnik, G., Fraile, R., 2019. Quantification of source specific black carbon scavenging using an aethalometer and a disdrometer. *Environ. Pollut.* 246, 336–345. doi:10.1016/j.envpol.2018.11.102.
- Blanco-Alegre, C., Castro, A., Calvo, A.I., Oduber, F., Alonso-Blanco, E., Fernández-González, D., Valencia-Barrera, R.M., Vega-Maray, A.M., Fraile, R., 2018. Below-cloud scavenging of fine and coarse aerosol particles by rain: the role of raindrop size. *Q. J. R. Meteorol. Soc.* 144, 2715–2726. doi:10.1002/qj.3399.
- Calvo, A.I., Pont, V., Olmo, F.J., Castro, A., Alados-Arboledas, L., Vicente, A.M., Fernández-Raga, M., Fraile, R., 2012. Air masses and weather types: a useful tool for characterizing precipitation chemistry and wet deposition. *Aerosol Air Qual. Res.* 12, 856–878. doi:10.4209/aaqr.2012.03.0068.
- Castro, A., Alonso-Blanco, E., González-Colino, M., Calvo, A.I., Fernández-Raga, M., Fraile, R., 2010. Aerosol size distribution in precipitation events in León. Spain. *Atmos. Res.* 96, 421–435. doi:10.1016/j.atmosres.2010.01.014.
- Celle-Jeanton, H., Travi, Y., Løye-Pilot, M.-D., Huneau, F., Bertrand, G., 2009. Rainwater chemistry at a mediterranean inland station (Avignon, France): local contribution versus long-range supply. *Atmos. Res.* 91, 118–126. doi:10.1016/j.atmosres.2008.06.003.
- Cheng, I., Zhang, L., 2017. Long-term air concentrations, wet deposition, and scavenging ratios of inorganic ions, HNO_3 , and SO_2 and assessment of aerosol and precipitation acidity at Canadian rural locations. *Atmos. Chem. Phys.* 17, 4711–4730. doi:10.5194/acp-17-4711-2017.
- Cugeron, K., De Michele, C., Ghezzi, A., Gianelle, V., 2018. Aerosol removal due to precipitation and wind forcings in Milan urban area. *J. Hydrol.* 556, 1256–1262. doi:10.1016/j.jhydrol.2017.06.033.
- Custódio, D., Cerqueira, M., Fialho, P., Nunes, T., Pio, C., Henriques, D., 2014. Wet deposition of particulate carbon to the Central North Atlantic ocean. *Sci. Total Environ.* 496, 92–99. doi:10.1016/j.scitotenv.2014.06.103.
- Draxler, R., Rolph, G., 2012. Hysplit (Hybrid Single-Particle Lagrangian Integrated Trajectory). Silver Spring. NOAA Air Resour. Lab.
- Dunn, O.J., 1964. Multiple comparisons using rank Sums. *Technometrics* 6, 241–252. doi:10.1080/00401706.1964.10490181.
- Encinas, D., Calzada, I., Casado, H., 2004. Scavenging ratios in an urban area in the Spanish Basque country. *Aerosol Sci. Technol.* 38, 685–691. doi:10.1080/02786820490460716.
- Favez, O., Cachier, H., Sciare, J., Alfaro, S.C., El-Araby, T.M., Harhash, M.A., Abdelwahab, M.M., 2008. Seasonality of major aerosol species and their transformations in Cairo megacity. *Atmos. Environ.* 42, 1503–1516. doi:10.1016/j.atmosenv.2007.10.081.
- Fernández-Raga, M., Castro, A., Marcos, E., Palencia, C., Fraile, R., 2017. Weather types and rainfall microstructure in Leon. Spain. *Int. J. Climatol.* 37, 1834–1842. doi:10.1002/joc.4816.
- Fernández-Raga, M., Castro, A., Palencia, C., Calvo, A.I., Fraile, R., 2009. Rain events on 22 October 2006 in León (Spain): drop size spectra. *Atmos. Res.* 93, 619–635. doi:10.1016/j.atmosres.2008.09.035.
- Fredericks, S., Saylor, J.R., 2019. Experimental study of drop shape and wake effects on particle scavenging for non-evaporating drops using ultrasonic levitation. *J. Aerosol Sci.* 127, 1–17. doi:10.1016/j.jaerosci.2018.10.001.
- Galindo, N., Nicolás, J.F., Yubero, E., Caballero, S., Pastor, C., Crespo, J., 2008. Factors affecting levels of aerosol sulfate and nitrate on the Western Mediterranean coast. *Atmos. Res.* 88, 305–313. doi:10.1016/j.atmosres.2007.11.024.

- Hastie, T., Tibshirani, R., Friedman, J., 2009. The Elements of Statistical Learning Data Mining, Inference, and Prediction, 2009. Springer series in statistics doi:10.1007/978-0-387-84858-7.
- He, J., Balasubramanian, R., 2008. Rain-aerosol coupling in the tropical atmosphere of Southeast Asia: distribution and scavenging ratios of major ionic species. *J. Atmos. Chem.* 60, 205–220. doi:10.1007/s10874-008-9118-x.
- Jaffrezo, J.-L., Colin, J.-L., 1988. Rain-aerosol coupling in urban area: scavenging ratio measurement and identification of some transfer processes. *Atmos. Environ.* 22, 929–935. doi:10.1016/0004-6981(88)90270-3.
- Jain, C.D., Madhavan, B.L., Ratnam, M.V., 2019. Source apportionment of rainwater chemical composition to investigate the transport of lower atmospheric pollutants to the UTLS region. *Environ. Pollut.* 248, 166–174. doi:10.1016/j.envpol.2019.02.007.
- Jordan, C.E., Dibb, J.E., Anderson, B.E., Fuelberg, H.E., 2003. Uptake of nitrate and sulfate on dust aerosols during TRACE-P. *J. Geophys. Res. Atmos.* 108, 1–10. doi:10.1029/2002jd003101.
- Kampa, M., Castanas, E., 2008. Human health effects of air pollution. *Environ. Pollut.* 151, 362–367. doi:10.1016/j.envpol.2007.06.012.
- Kasper-Giebl, A., Kalina, M.F., Puxbaum, H., 1999. Scavenging ratios for sulfate, ammonium and nitrate determined at Mt. Sonnblick (3106m a.s.l.). *Atmos. Environ.* 33, 895–906. doi:10.1016/S1352-2310(98)00279-9.
- Keene, W.C., Pszenny, A.A.P., Galloway, J.N., Hawley, M.E., 1986. Sea-salt corrections and interpretation of constituent ratios in marine precipitation. *J. Geophys. Res.* 91, 6647. doi:10.1029/JD091iD06p06647.
- Keresztesi, Á., Korodi, A., Boga, R., Petres, S., Ghita, G., Ilie, M., 2017. Chemical characteristics of wet precipitation in the Eastern Carpathians. Romania. *Ecoterra* 14, 52–59.
- Knote, C., Hodzic, A., Jimenez, J.L., 2015. The effect of dry and wet deposition of condensable vapors on secondary organic aerosols concentrations over the continental US. *Atmos. Chem. Phys.* 15, 1–18. doi:10.5194/acp-15-1-2015.
- Kruskal, W.H., Wallis, W.A., 1952. Use of ranks in one-criterion variance analysis. *J. Am. Stat. Assoc.* 47, 583–621. doi:10.1080/01621459.1952.10483441.
- Kulshrestha, U.C., Kulshrestha, M.J., Sekar, R., Sastry, G.S.R., Vairamani, M., 2003. Chemical characteristics of rainwater at an urban site of south-central India. *Atmos. Environ.* 37, 3019–3026. doi:10.1016/S1352-2310(03)00266-8.
- Kulshrestha, U.C., Reddy, L.A.K., Satyanarayana, J., Kulshrestha, M.J., 2009. Real-time wet scavenging of major chemical constituents of aerosols and role of rain intensity in Indian region. *Atmos. Environ.* 43, 5123–5127. doi:10.1016/j.atmosenv.2009.07.025.
- Kulshrestha, U.C., Sarkar, A.K., Srivastava, S.S., Parashar, D.C., 1996. Investigation into atmospheric deposition through precipitation studies at New Delhi (India). *Atmos. Environ.* 30, 4149–4154. doi:10.1016/1352-2310(96)00034-9.
- Kulshrestha, U.C., Sarkar, A.K., Srivastava, S.S., Parashar, D.C., 1995. Wet-only and bulk deposition studies at New Delhi (India). *Water, Air, Soil Pollut.* 85, 2137–2142. doi:10.1007/BF01186150.
- Lamb, H.H., 1972. British Isles weather types and a register of daily sequence of circulation patterns, geophysical memoir, HMSO, London. Her Majesty's stationery office.
- Lelieveld, J., Evans, J.S., Fnais, M., Giannadaki, D., Pozzer, A., 2015. The contribution of outdoor air pollution sources to premature mortality on a global scale. *Nature* 525, 367–371. doi:10.1038/nature15371.
- Luan, T., Guo, X., Zhang, T., Guo, L., 2019. Below-cloud aerosol scavenging by different-intensity rains in Beijing city. *J. Meteorol. Res.* 33, 126–137. doi:10.1007/s13351-019-8079-0.
- Lucarelli, F., Chiari, M., Calzolari, G., Giannoni, M., Nava, S., Udisti, R., Severi, M., Querol, X., Amato, F., Alves, C., Eleftheriadis, K., 2015. The role of PIXE in the AIRUSE project "testing and development of air quality mitigation measures in Southern Europe. *Nucl. Instrum. Methods Phys. Res. Sect. B Beam Interact. Mater. Atoms* 363, 92–98. doi:10.1016/j.nimb.2015.08.023.
- Mage, D., Ozolins, G., Peterson, P., Webster, A., Orthofer, R., Vandeweerde, V., Gwynne, M., 1996. Urban air pollution in the mega-cities of the world. *Atmos. Environ.* 30, 681–686.
- Martins, E.H., Nogarotto, D.C., Mortatti, J., Pozza, S.A., 2019. Chemical composition of rainwater in an urban area of the southeast of Brazil. *Atmos. Pollut. Res.* 10, 520–530. doi:10.1016/j.apr.2018.10.003.
- Mori, T., Kondo, Y., Ohata, S., Moteki, N., Matsui, H., Oshima, N., Iwasaki, A., 2014. Wet deposition of black carbon at a remote site in the East China Sea. *J. Geophys. Res. Atmos.* 119, 10485–10498. doi:10.1002/2014JD022103.
- Naddafi, K., Hassanvand, M.S., Yunesian, M., Momeniha, F., Nabizadeh, R., Faridi, S., Gholampour, A., 2012. Health impact assessment of air pollution in megacity of Tehran. *Iranian J. Environ. Health Sci. Eng.* 9, 28. doi:10.1186/1735-2746-9-28.
- Oduber, F., Calvo, A.I., Blanco-Alegre, C., Castro, A., Nunes, T., Alves, C., Sorribas, M., Fernández-González, D., Vega-Maray, A.M., Valencia-Barrera, R.M., Lucarelli, F., Nava, S., Calzolari, G., Alonso-Blanco, E., Fraile, B., Fialho, P., Coz, E., Prevot, A.S.H., Pont, V., Fraile, R., 2019a. Unusual winter Saharan dust intrusions at Northwest Spain: air quality, radiative and health impacts. *Sci. Total Environ.* 669, 213–228. doi:10.1016/j.scitotenv.2019.02.305.
- Oduber, F., Calvo, A.I., Blanco-Alegre, C., Castro, A., Vega-Maray, A.M., Valencia-Barrera, R.M., Fernández-González, D., Fraile, R., 2019b. Links between recent trends in airborne pollen concentration, meteorological parameters and air pollutants. *Agric. For. Meteorol.* 264, 16–26. doi:10.1016/j.agrformet.2018.09.023.
- Oduber, F., Calvo, A.I., Castro, A., Blanco-Alegre, C., Alves, C., Barata, J., Nunes, T., Lucarelli, F., Nava, S., Calzolari, G., Cerqueira, M., Martín-Villacorta, J., Esteves, V., Fraile, R., 2020. Chemical composition of rainwater under two events of aerosol transport: a Saharan dust outbreak and wildfires. *Sci. Total Environ.* 734, 139202. doi:10.1016/j.scitotenv.2020.139202.
- Oduber, F., Calvo, A.I., Castro, A., Blanco-Alegre, C., Alves, C., Calzolari, G., Nava, S., Lucarelli, F., Nunes, T., Barata, J., Fraile, R., 2021. Characterization of aerosol sources in León (Spain) using positive matrix factorization and weather types. *Sci. Total Environ.* doi:10.1016/j.scitotenv.2020.142045.
- Oduber, F., Castro, A., Calvo, A.I., Blanco-Alegre, C., Alonso-Blanco, E., Belmonte, P., Fraile, R., 2018. Summer-autumn air pollution in León, Spain: Changes in aerosol size distribution and expected effects on the respiratory tract. *Air Qual. Atmos. Heal.* 11, 505–520. doi:10.1007/s11869-018-0556-6.
- Olzowski, T., 2014. The efficiency of PM10 scavenging from troposphere as a function of type and duration of wet deposition, in: Fiore, S. (Ed.), 1st international conference on atmospheric dust- DUST2014. pp. 393–398. doi:10.14644/dust.2014.064
- Olzowski, T., Ziemcik, Z., 2018. An alternative conception of PM10 concentration changes after short-term precipitation in urban environment. *J. Aerosol Sci.* 121, 21–30. doi:10.1016/j.jaerosci.2018.04.001.
- Pan, Y.P., Wang, Y.S., 2015. Atmospheric wet and dry deposition of trace elements at 10 sites in Northern China. *Atmos. Chem. Phys.* 15, 951–972. doi:10.5194/acp-15-951-2015.
- Pio, C., Cerqueira, M., Harrison, R.M., Nunes, T., Mirante, F., Alves, C., Oliveira, C., Sanchez de la Campa, A., Artifano, B., Matos, M., 2011. OC/EC ratio observations in Europe: re-thinking the approach for apportionment between primary and secondary organic carbon. *Atmos. Environ.* 45, 6121–6132. doi:10.1016/j.atmosenv.2011.08.045.
- Querol, X., Alastuey, A., Viana, M.M., Rodriguez, S., Artifano, B., Salvador, P., Garcia do Santos, S., Fernandez Patier, R., Ruiz, C.R., de la Rosa, J., Sanchez de la Campa, A., Menendez, M., Gil, J.L., 2004. Speciation and origin of PM10 and PM2.5 in Spain. *J. Aerosol Sci.* 35, 1151–1172. doi:10.1016/j.jaerosci.2004.04.002.
- Ren-Jian, Z., Kin-Fai, H., Zhen-Xing, S., 2012. The role of aerosol in climate change, the environment, and human health. *Atmos. Ocean. Sci. Lett.* 5, 156–161. doi:10.1080/16742834.2012.11446983.
- Rolph, G., Stein, A., Stunder, B., 2017. Real-time environmental applications and display system: READY. *Environ. Model. Softw.* 95, 210–228. doi:10.1016/j.envsoft.2017.06.025
- Roy, A., Chatterjee, A., Ghosh, A., Das, S.K., Ghosh, S.K., Raha, S., 2019. Below-cloud scavenging of size-segregated aerosols and its effect on rainwater acidity and nutrient deposition: a long-term (2009–2018) and real-time observation over eastern Himalaya. *Sci. Total Environ.* 674, 223–233. doi:10.1016/j.scitotenv.2019.04.165.
- Sanets, E.V., Chuduk, V.N., 2005. Sulphur atmospheric deposition in areas with different anthropogenic loads in Belarus. *Atmos. Res.* 77, 88–99. doi:10.1016/j.atmosres.2004.10.019.
- Seinfeld, J.H., Pandis, S.N., 2016. Atmospheric Chemistry and Physics: From Air Pollution to Climate Change. 3rd ed. John Wiley & Sons.
- Śliudek, P., Frankowski, M., Siepak, J., 2015. Seasonal variations of dissolved organic carbon in precipitation over urban and forest sites in central Poland. *Environ. Sci. Pollut. Res.* 22, 11087–11096. doi:10.1007/s11356-015-4356-3.
- Stein, A.F., Draxler, R.R., Rolph, G.D., Stunder, B.J.B., Cohen, M.D., Ngan, F., 2015. NOAA's HYSPLIT atmospheric transport and dispersion modeling system. *Bull. Am. Meteorol. Soc.* 96, 2059–2077. doi:10.1175/BAMS-D-14-00110.1.
- Theodosi, C., Im, U., Bougiatioti, A., Zarmas, P., Yenigun, O., Mihalopoulos, N., 2010. Aerosol chemical composition over Istanbul. *Sci. Total Environ.* 408, 2482–2491. doi:10.1016/j.scitotenv.2010.02.039.
- Trigo, R.M., DaCamara, C.C., 2000. Circulation weather types and their influence on the precipitation regime in Portugal. *Int. J. Climatol.* 20, 1559–1581. doi:10.1002/1097-0088(200011)20:13<1559::AID-JOC555>3.0.CO;2-5.
- Uchiyama, R., Okochi, H., Katsumi, N., Ogata, H., 2017. The impact of air pollutants on rainwater chemistry during "urban-induced heavy rainfall" in downtown Tokyo. *Japan. J. Geophys. Res. Atmos.* 122, 6502–6519. doi:10.1002/2017JD026803.
- Vicente, A., Alves, C., Calvo, A.I., Fernandes, A.P., Nunes, T., Monteiro, C., Almeida, S.M., Pio, C., 2013. Emission factors and detailed chemical composition of smoke particles from the 2010 wildfire season. *Atmos. Environ.* 71, 295–303. doi:10.1016/j.atmosenv.2013.01.062.
- Vicente, A., Alves, C., Monteiro, C., Nunes, T., Mirante, F., Cerqueira, M., Calvo, A., Pio, C., 2012. Organic speciation of aerosols from wildfires in central Portugal during summer 2009. *Atmos. Environ.* 57, 186–196. doi:10.1016/j.atmosenv.2012.04.030.
- Xu, D., Ge, B., Wang, Z., Sun, Y., Chen, Y., Ji, D., Yang, T., Ma, Z., Cheng, N., Hao, J., Yao, X., 2017. Below-cloud wet scavenging of soluble inorganic ions by rain in Beijing during the summer of 2014. *Environ. Pollut.* 230, 963–973. doi:10.1016/j.envpol.2017.07.033.
- Zhang, M., Wang, S., Wu, F., Yuan, X., Zhang, Y., 2007. Chemical compositions of wet precipitation and anthropogenic influences at a developing urban site in southeastern China. *Atmos. Res.* 84, 311–322. doi:10.1016/j.atmosres.2006.09.003.
- Zikova, N., Zdimal, V., 2016. Precipitation scavenging of aerosol particles at a rural site in the Czech Republic. *Tellus B Chem. Phys. Meteorol.* 68, 27343. doi:10.3402/tellusb.v68.27343.